Journal of Electronic Materials
https://doi.org/10.1007/s11664-025-12194-x

ORIGINAL RESEARCH ARTICLE

Comparative Study of Dye-Sensitized Solar Cells with Natural Dye Extracts of *Vernonia amygdalina*, *Goeppertia macrosepala* Leaves, and *Cnestis ferruginea* Fruit as Photosensitizers

Ayodele O. Soge[1] · Abayomi F. Oshin[1] · Christoph Ulbricht[2] · Felix Mayr[2] · Olumide D. Olukanni[3] · Oluropo F. Dairo[4] · Modupe E. Sanyaolu[1] · Olalere G. Adeyemi[5] · Serpil Tekoglu[2] · Markus C. Scharber[2] · Alexander A. Willoughby[1]

Received: 24 December 2024 / Accepted: 30 June 2025

Abstract

As photosensitizers for harvesting solar energy, dyes play a major role in the operation and photochemical performance of dye-sensitized solar cells (DSSCs). DSSCs are usually fabricated using non-biodegradable, synthetic dyes, which often contain toxic heavy metals. However, replacing synthetic dyes with cheap and biodegradable natural dyes can produce cost-effective and eco-friendly DSSCs. In this study, we investigate the suitability of natural dye extracts of *Vernonia amygdalina*, *Goeppertia macrosepala* leaves and *Cnestis ferruginea* fruit as photosensitizers in DSSCs. The influence of solvents on the performance of these three natural dye extracts is also examined. The natural dyes are extracted using acetone and ethanol solvents and characterized by Fourier-transform infrared (FTIR), UV–Vis, and photoluminescence (PL) spectroscopy. The FTIR spectrometry results for all the dye samples demonstrate the presence of three functional groups: the hydroxyl, amine, and carbonyl groups, a strong indication of good adsorption by the semiconductor metal oxides in DSSCs. The UV-Vis and PL spectra show that the natural dyes of *V. amygdalina*, *G. macrosepala*, and *C. ferruginea* extracted with acetone and ethanol exhibit stable and strong optical absorption in the visible region of the electromagnetic spectrum. Thus, the three natural dyes examined are potential candidates for photosensitizers in DSSCs. The DSSC fabricated with *V. amygdalina* dye extracted using acetone delivers the highest solar conversion efficiency with performance parameters J_{sc}, V_{oc}, *FF*, and η as 330.51 μA/cm^2, 522 mV, 0.7, and 0.12%, respectively. A higher solar efficiency is recorded by chlorophyll-based dyes of *V. amygdalina* and *G. macrosepala* leaves than anthocyanin-based dye of *C. ferruginea* fruit. Acetone-extracted dye samples outperform samples using ethanol as the solvent for dye extraction from *V. amygdalina* and *G. macrosepala*. The three natural dyes displayed a lower electrical performance than the synthetic ruthenium-based dye ($\eta = 2.84\%$) due to their

✉ Ayodele O. Soge
sogea@run.edu.ng; ayosoge@gmail.com

[1] Department of Physical Sciences, Faculty of Natural Sciences, Redeemer's University, PMB 230, Akoda, Ede 232102, Osun State, Nigeria

[2] Linz Institute for Organic Solar Cells (LIOS), Institute of Physical Chemistry, Johannes Kepler University Linz, Altenberger Straße 69, 4040 Linz, Austria

[3] Department of Biochemistry, Faculty of Basic Medical Sciences, Redeemer's University, PMB 230, Akoda, Ede 232102, Osun State, Nigeria

[4] Department of Electrical and Electronic Engineering, Faculty of Engineering, Redeemer's University, PMB 230, Akoda , Ede 232102, Osun State, Nigeria

[5] Department of Chemical Sciences, Faculty of Natural Sciences, Redeemer's University, PMB 230, Akoda, Ede 232102, Osun State, Nigeria

Published online: 24 July 2025

inherent challenges: narrow absorption spectra attributed to their less-optimized molecular structures, poor photostability under prolonged illumination, slow electron injection rates, and high recombination losses.

Graphical Abstract

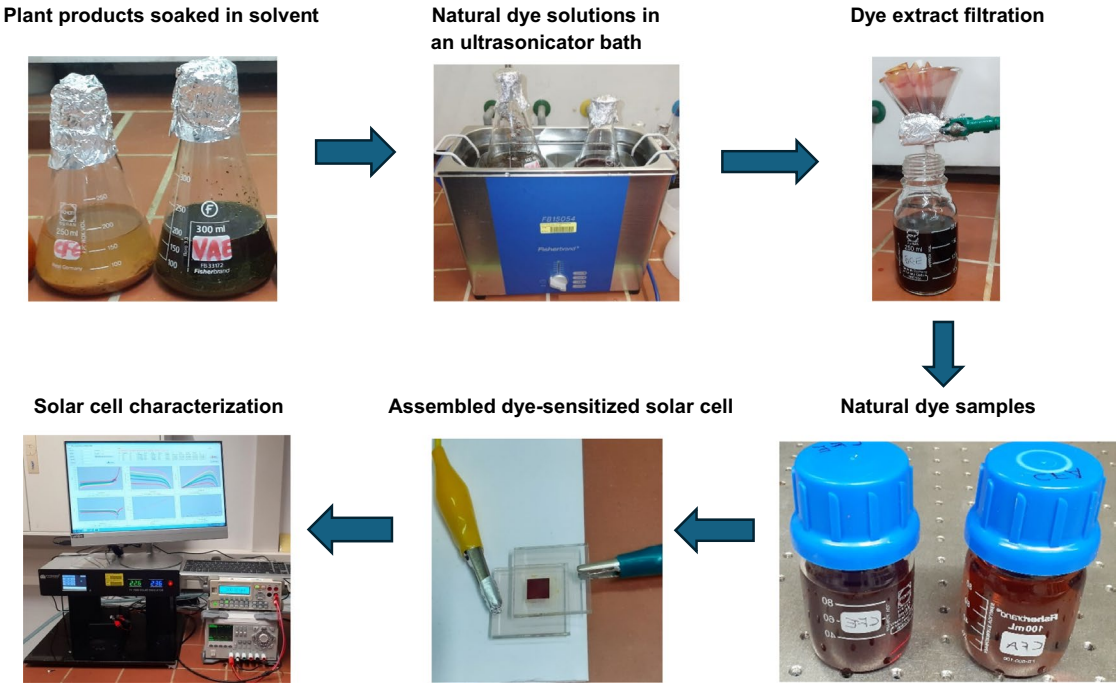

Keywords Solar energy · synthetic dyes · natural dyes · dye-sensitized solar cells · photosensitizers · power conversion efficiency

Introduction

Solar energy has become a prominent renewable energy source in the twenty-first century due to its practically endless supply and non-polluting nature, unlike fossil resources: coal, petroleum, and natural gas.[1] Over the years, several photovoltaic technologies have been developed to harvest solar energy to meet the rising global demand for clean, affordable, and sustainable energy. Examples of such photovoltaic technologies are monocrystalline silicon cells, polycrystalline silicon cells, perovskite cells, organic solar cells, thin-film solar cells, dye-sensitized solar cells (DSSCs), and quantum dot cells. DSSCs have the potential to be a viable alternative to today's regularly used silicon cells due to several promising advantages over silicon-based cells, such as lower cost, use of non-toxic materials, ease of production, and flexible substrates.[2] In addition, a DSSC can be fabricated as an eco-friendly device without toxic materials, unlike perovskite solar cells, which usually contain toxic lead, and organic solar cells, which require highly toxic solvents for preparation.[2] DSSCs are suitable energy sources for portable electronics because they can be manufactured as thin and lightweight flexible devices.[3] In typical indoor conditions, DSSCs exhibit a higher efficiency under dim light than conventional silicon-based PV technologies, thereby qualifying them as potential candidates for ambient energy harvesting for the wireless sensors utilized in the Internet of Things (IoT) devices.[3–5]

Furthermore, DSSCs show significant potential for integration into wearable electronics. Utilizing ambient light, DSSCs can offer a renewable energy source for various wearable technologies such as smartwatches, fitness trackers, smart clothing, and health monitoring systems. In agrivoltaic systems, low efficiency remains a concern for large-scale energy output, yet DSSCs may provide shading in greenhouses for light-tolerant crops, potentially reducing internal temperatures.[6] Moreover, DSSCs can power IoT sensors for monitoring environmental conditions.

A typical DSSC comprises two conductive electrodes, a photoanode coated with a porous metal oxide semiconductor, such as TiO_2, ZnO, or SnO_2, and a counter electrode (or cathode) coated with an electrocatalyst, usually platinum or graphite.[7,8] The semiconductor is also covered with a photoactive dye to harvest sunlight for conversion

into electrical energy. In a fully assembled DSSC, the two electrodes assume a sandwich-like structure with an electrolyte solution injected in between them. Electrolytes based on redox couples, for example, iodine/triiodide, are commonly used electrolytes in DSSCs.[7]

The power conversion efficiency (PCE) of a DSSC largely depends on the photochemical performance of the dye used as a photosensitizer to harvest the sunlight.[9] A wide absorption spectrum, coupled with lower cost and energy level matching to semiconductor materials, are required to qualify as the best dye material.[8] Ruthenium-based synthetic dyes such as N719 and N3 have given comparatively high PCEs for dye-sensitized solar cells of 10% and 11.2%, respectively.[10] However, high processing costs due to complex synthetic procedures and the huge environmental impact of heavy metals have limited the further use of these Ru-based dyes for DSSC applications.[8–12] Instead, natural dyes extracted from the leaves, flowers, and fruits of plants have been widely investigated owing to their environmental sustainability, low cost, widespread availability, low-temperature processing, and facile synthesis.[9,13,14] Nevertheless, improvement in solar cell efficiency has been progressive in the literature but at a slow pace[15,16] . According to Kohn et al.,[2] the typical efficiencies for solar cells with natural dyes as photosensitizers were between 0.0002 and 2.3%. Hence, the search for efficient charge-injecting dye is crucial for a breakthrough in DSSCs research since the dyes are the electron-injecting matter in the circuit of DSSCs. As part of the effort to optimize natural dyes, Kabir et al.[17] fabricated DSSCs using betalain and curcumin as photosensitizers and obtained PCEs of 0.22% and 0.47%, respectively. Similarly, Siregar et al.[18] reported a maximum efficiency of 3.53% for a DSSC sensitized with rose myrtle (*Rhodomyrtus tomentosa*) fruit extract.

Sowmya et al.[19] extracted natural dyes from fresh and dried henna (*Lawsonia inermis*) leaves using different solvents, namely acetone, ethanol, and distilled water. The extracts were used as photosensitizers in six different solar cells and were characterized using UV-Vis and Fourier-transform infrared (FTIR) spectroscopy. The authors discovered that the dye extracted from the dried leaves utilizing acetone as a solvent had the best efficiency of 0.351% with a fill factor of 0.3765 compared to the other cells. Likewise, Ali et al.[20] investigated the natural dye extract of blackberry as a photosensitizer in DSSCs. An efficiency of 0.26% was delivered by the DSSC fabricated with TiO_2 as the photoanode.

Furthermore, Yadav et al. [21] utilized four different natural dye extracts derived from butea monosperm, crown of thorns, red lantana camara, and royal poinciana flowers as photosensitizers in DSSCs. According to the authors, the highest PCE of 2.89% was obtained for the device fabricated with the natural dye extract of butea monosperm as a photosensitizer. This is the highest PCE ever reported for the device using the natural dye of butea monosperm flower as photosensitizer. Hence, the natural dye extracts of butea monosperm are a suitable eco-friendly and low-cost replacement for synthetic dyes.

Similarly, Mahapatra et al.[22] compared the photochemical performances of DSSCs using natural dye extracts from three inedible plants—*Bixa orellana* seeds, *Mallotus phillipensis* pericalp fruits, and *Basella alba* ripe fruits—as photosensitizers in DSSCs. The fabricated solar devices delivered a PCE of 0.67% for *Bixa orellana*, 0.55% for *Mallotus phillipensi*, and 0.32% *Basella alba.* Thus, *Bixa orellana* dye extract-based solar cells possessed the best efficiency with an open-circuit voltage of 0.51 V, a short-circuit current density of 2.13 mA/cm^2, and a fill factor of 62% in conformity with the computational results. Based on their biocompatibility, easy availability, and low cost, the natural dye extracts of *Bixa orellana* are potential alternatives for toxic and expensive synthetic dyes. Moreover, Flint et al.[23] investigated betanin dye extracted from ayrampo seeds of the Peruvian-native prickly pear (*Opuntia soehrensii*) as a photosensitizer in DSSCs. The photosensitive dye was stabilized by adding citric acid to enhance the performance of the solar cells. A PCE of 1.41% was recorded which increased to 4% under low-light condition. Likewise, Rakshit et al.[24] studied the effect of TiO_2 nanoparticles on the electrical transport properties of betanin dye extracted from red beetroot (*Beta vulgaris*). A notable increase in conductivity from 6.16 to 2.03×10^{-8} $(\Omega\ cm)^{-1}$ was recorded when the nanoparticles were integrated into the dye at room temperature. Effective mobility also increased from 1.236 to 4.069×10^{-4} $cm^2v^{-1}\ s^{-1}$ in the presence of TiO_2 nanoparticles.

Titania (TiO_2) is commonly used as photoanode material in DSSCs due to its high electron mobility, compatibility with dyes, tunable properties, and chemical stability. Hence, the photochemical performance of a DSSC can be enhanced by modifying TiO_2 using co-adsorbents such as chenodeoxycholic acid, which inhibits dye molecules from aggregating on the TiO_2 surface. Mass aggregation of dye molecules causes a high rate of electron recombination at the dye/TiO_2 interface, which reduces electron injection into the conduction band of the TiO_2. Incorporating co-adsorbents in TiO_2 increases its dye loading capacity, which improves the electron injection efficiency and decreases recombination losses.[25] As an alternative to TiO_2, ZnO with similar electron affinity (~ 3.2 eV) and bandgap energy (~ 3.3 eV) to TiO_2, coupled with its low cost and stability to photo-corrosion, has been reported to be a suitable photoanode material for DSSCs.[26] Among other attractive features that ZnO offers for photovoltaic applications are a greater electron diffusivity than TiO_2, a remarkable excitation binding energy of 60 eV, and a large electron mobility of 115–155 cm^2/Vs. Therefore, several researchers have explored ZnO-based DSSCs with

excellent results ascribed to the efficient electron transport of this semiconductor, leading to reduced recombination reactions in the photovoltaic cell.[27,28] For instance, Maruccia et al.[26] reported aqueous DSSCs fabricated with three different ZnO electrode morphologies comprising nanoparticles, desert roses, and multipods. Desert roses' morphology delivered the most efficient DSSCs, attributed to their high specific surface area for dye adsorption and suitable particle interconnection for electron transport.

As a measure to overcome the challenge of charge carrier recombination in TiO_2-based DSSCs and, consequently, improving the PCE of the solar cells, Ndlovu et al.[29] proposed reduced graphene oxide (rGO)–$Sr_{0.7}Sm_{0.3}Fe_{0.6}Co_{0.4}O_3$ (rGO-SSFC) nanocomposites as potential photoanodes for DSSCs. An improved open-circuit voltage of 0.84 V, a short-circuit current density of 14.02 mA/cm^2, and a PCE of 7.25% were obtained. Similarly, to improve the light-harvesting efficiency of photoanodes towards boosting the PCE of DSSCs, Dharani et al.[30] investigated rGO/Ce-Zn_2SnO_4 nanocomposites as possible alternatives for TiO_2 in DSSCs, and the results revealed that DSSCs fabricated with Ce-doped Zn_2SnO_4/rGO photoanodes exhibited enhanced photovoltaic properties with a PCE of 7.19%, an open-circuit voltage of 0.85 V, a short-circuit current density of 15.86 mA cm^{-2}, and a fill factor of 0.74. Therefore, material modification is an effective approach for enhancing the photovoltaic performance of DSSCs.

Moreover, Shan et al.[31] explored the co-sensitization technique by mixing betalain and anthocyanin natural dye extracts of beetroot and cranberries, respectively, as a measure to improve the panchromatic light-harvesting and photovoltaic performance of DSSCs. An improved performance was obtained from the mixed-dye-based DSSCs compared to the single-dye-based DSSCs, and produced a short-circuit current density, an open-circuit voltage, and a fill factor of 0.36 mA/cm^2, 0.42 V, and 0.51, respectively. The maximum efficiency of the mixed-dye-based DSSCs was 5.37 and 1.16 times higher than that of beetroot and cranberry dye-based DSSCs, respectively. Therefore, combining two or more natural dyes can result in good sensitization and enhanced photovoltaic performance towards achieving more efficient DSSCs.

Similarly, Chang et al.[32] reported a maximum efficiency of 0.72% using a mixture of chlorophyll and anthocyanin dyes from promegranate leaves and mulberry organic products, respectively. However, the fabricated DSSC delivered an efficiency of 0.60% and 0.55%, respectively, when chlorophyll and anthocyanin dyes were utilized. Thus, the co-sensitization technique enhanced the performance of the single-dye-based DSSCs.

In this study, we have compared the photochemical performance of the natural dye extracts of bitter leaf (*Vernonia amygdalina*), calathea (*Goeppertia macrosepala*) leaves, and wild alder (*Cnestis ferruginea*) fruit as photosensitizers in DSSCs. The influence of solvents on the performance of these three natural dye extracts in DSSCs has also been investigated.

Materials and Methods

Materials

The materials for DSSC fabrication were procured from Solaronix (Switzerland), which include N719 dye, fluorine-doped tin oxide (FTO) electrodes coated with platinum (Pt), an electrolyte (Iodolyte AN-50), FTO electrodes layered with titania (TiO_2), and gaskets. Solvents for dye extraction comprising ethanol, methanol, and acetone were purchased from Merck (Germany). Samples of bitter leaf (*V. amygdalina*), calathea (*G. macrosepala*) leaves, and wild alder (*C. ferruginea*) fruit (Fig. 1) were collected from the farm for dye extraction by direct method using solvents.

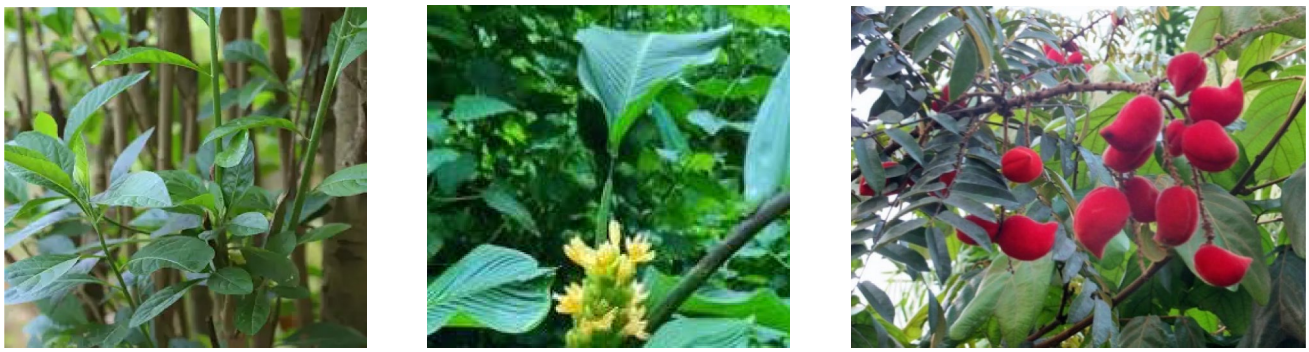

(a) (b) (c)

Fig. 1 (a) Bitter leaf (*V. amygdalina*), (b) calathea (*G. macrosepala*) leaves, and (c) wild alder (*C. ferruginea*) fruit.

As the name implies, bitter leaf has a bitter taste but is widely used as a main vegetable in soups and stews of diverse cultures in Africa. It also has several medicinal benefits, including treating feverish conditions, malaria, diabetes, high blood pressure, prostate cancer, inflammation, and infertility.[33,34] Likewise, *G. macrosepala* is useful for ornamental purposes and traditional medicine, and its dried tuberous roots are sources of starch and protein.[35] *C. ferruginea* is used for oral hygiene and in traditional African medicine as an anti-convulsant, analgesic, antimicrobial, laxative, and anti-oxidant, and for treating infections such as dysentery, bronchitis, conjunctivitis, and sinusitis.[36]

The chemical structure of chlorophyll—the pigment contained in *V. amygdalina* and *G. macrosepala* leaves—is shown in Fig. 2a. There are several pigment varieties of chlorophyll, which are classified based on their molecular structure and absorption spectra. The most common form is chlorophyll-a, which is responsible for absorbing blue and red light. It comprises a chlorine ring plus a magnesium center and several side chains with hydrocarbon traces,[37,38] as depicted in Fig. 2a. The various chlorophyll pigment varieties play a specific role in photosynthesis by absorbing different parts of the light spectrum to energize the process. Chlorophyll can absorb red, blue, and violet wavelengths and reflect them in green.[37] In addition, chlorophyll converts solar energy into chemical energy and participates in electron transfers. *C. ferruginea* fruit contains a pigment called ferruginin, which is a type of anthocyanin, a class of flavonoids responsible for the purple-red pigment commonly found in fruits, leaves, flowers, roots, and sprouts.[37] The chemical structure of anthocyanin pigment, as illustrated in Fig. 2b, comprises 15 carbon atoms, 3 carbon bridges, and 2 phenyl rings.

Dye Extraction Process and Characterization

Samples of *V. amygdalina* leaves (chlorophyll pigment), *G. macrosepala* leaves (chlorophyll pigment), and *C. ferruginea* fruit (anthocyanin pigment) were washed with normal water and later rinsed with distilled water for dye extraction using the cold extraction method.[39] The samples were dried for 5 days at room temperature and blended separately using a blender. The ground samples were weighed differently using a weighing balance and wholly immersed into two solvents, acetone and ethanol. Afterward, 25 g each of *V. amygdalina* ground leaves were soaked in 150 ml of acetone and ethanol separately, and labeled as VAA and VAE samples, respectively. Likewise, 25 g each of *G. macrosepala* ground leaves were immersed in 150 ml of acetone and ethanol separately and labeled as GMA and GME samples, respectively. Also, 25 g each of ground *C. ferruginea* fruit were soaked in 150 ml of acetone and ethanol separately, and categorized as CFA and CFE samples, respectively. Moreover, 2 ml of concentrated hydrochloric acid (HCl) was added

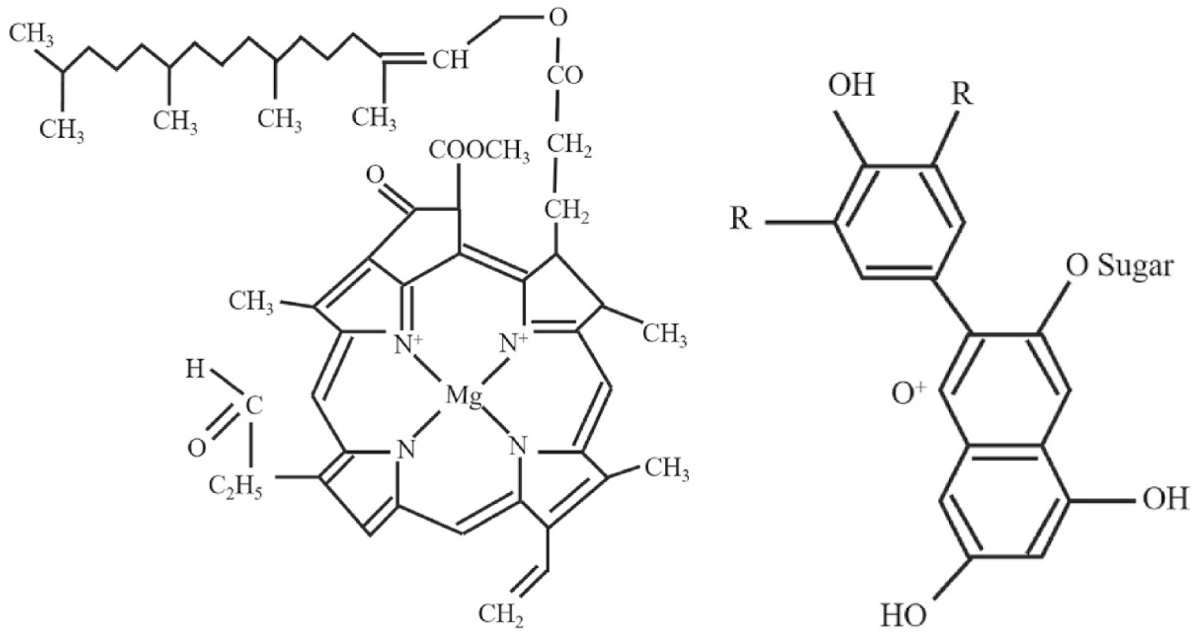

Fig. 2 The chemical structure of (a) chlorophyll and (b) anthocyanin pigments. Reprinted from reference [37], under the terms of the Creative Commons CC-BY-NC-ND 4.0 licence, available at https://creativecommons.org/licenses/by-nc-nd/4.0/deed.en.

to all the samples soaked in the different solvents in their respective conical flasks to acidify the solution. An acidified solution promotes the acid hydrolysis of the plant cells, as acid hydrolysis breaks down the bonds of the plant cell wall for increased pigmentation release. The sample solutions in each assigned beaker were sonicated in an aluminum alloy rectangular ultra-bath sonicator machine, as shown in Fig. 3a. Sonication of the plant sample involves using an ultrasonic frequency to set the particles of the plant samples into vibration to enhance pigment extraction from them. Following the sonication process, the dye extracts were filtered and appropriately stored in well-labeled containers for easy future identification, as displayed in Fig. 3b.

Furthermore, the natural dye extracts of *V. amygdalina*, *G. macrosepala* leaves, and *C. ferruginea* fruit were characterized using a PerkinElmer Lambda 1050 spectrophotometer to measure their optical absorbance in the ultraviolet and visible regions of the electromagnetic spectrum. The UV-spectrophotometer can determine specific wavelengths absorbed by a dye extract in the visible light spectrum range (400–750 nm) and the ultraviolet spectrum range (200–400 nm). The spectral absorbance range of the three natural dye extracts was measured between 200 and 750 nm, and the resulting spectrum data were analyzed.

(a)

(b)

Fig. 3 (a) Natural dye extracts in an ultra-bath sonicator machine, and (b) natural dye samples of *V. amygdalina* leaves (labeled *VAA* and *VAE*), *G. macrosepala* leaves (*GMA* and *GME*), and *C. ferruginea* fruit (*CFA* and *CFE*) extracted with acetone and ethanol, respectively. The last letter of the label (A or E) represents the extraction solvent (acetone or ethanol), while the first two letters of the labels (VA, GM, and CF) are the acronyms for the plant names.

Photoluminescence (PL) spectra of the three natural dye extracts were also measured from the same solutions used in UV-Vis absorption spectroscopy on a PTI QuantaMaster 40 photoluminescence spectrometer. FTIR spectroscopy analysis was performed to determine the chemical compositions of the natural dye extracts using a Bruker Vertex 80 FTIR spectrometer.

Solar Cell Fabrication and Measurements

The DSSCs were fabricated using three natural dyes extracted from *V. amygdalina*, *G. macrosepala* leaves, and *C. ferruginea* fruit as photosensitizers. The photoanodes comprised FTO glass substrates with a printed layer of titania (TiO_2) nanoparticles. The TiO_2 electrode with a dimension of 6 mm x 6 mm had an active cell area of 0.36 cm^2 covered by the TiO_2 film. The photoanodes were stained with natural dyes by immersing them in dyes with the TiO_2 film facing upward to prevent scratching the TiO_2 surface. To aid the natural adsorption of the dye molecules onto the TiO_2 particles, the photoanodes were immersed in the dye solutions for 24 h. The stained TiO_2 electrodes were rinsed in deionized water to eliminate excess dye before drying at room temperature.

The counter electrodes, consisting of drilled FTO glass substrates coated with platinum, were blown with nitrogen air to clean the surface. The conductive side of the Pt-coated FTO substrate was determined using a digital multimeter (RS927A). The photoanode and counter electrode were laminated together using a gasket made of a thin polymer film. The Pt-coated counter electrode was positioned on a TiO_2-coated photoanode with a small hole in the counter electrode at the center of the TiO_2 layer. The conductive sides of the two FTO substrates were arranged to face each other with a little offset for electrical contacts. The two electrodes were pressed together for the gasket to stick to both electrodes before the assembled solar cell was placed on a hot plate at 120 °C to melt the gasket. The solar cell was later sealed using a hot iron rod to press the two electrodes together for a few seconds until they became airtight. The sealed cell was removed from the hot plate and allowed to cool. The cavity formed by the sealing gasket between the two sealed electrodes was then filled with the electrolyte. Some drops of iodine/triiodide electrolyte (Iodolyte AN-50) were injected into the created chamber between the two electrode glass substrates via the drilled hole in the counter electrode, which was then sealed using a small glass cap placed on a gasket to prevent electrolyte leakage and moisture from degrading the cell. The fabricated dye-sensitized solar cell is shown in Fig. 4a.

For comparison purposes, a reference cell was also fabricated using a synthetic ruthenium-based dye, known as N719 dye. This synthetic dye was prepared by dissolving

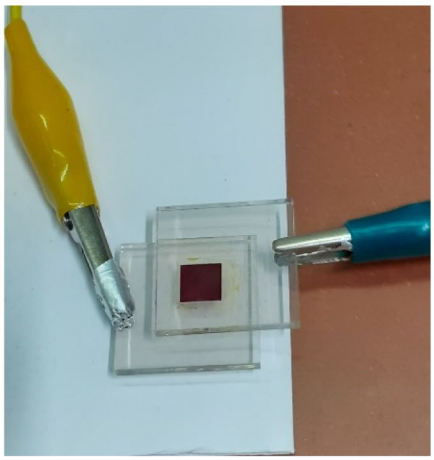

(a)

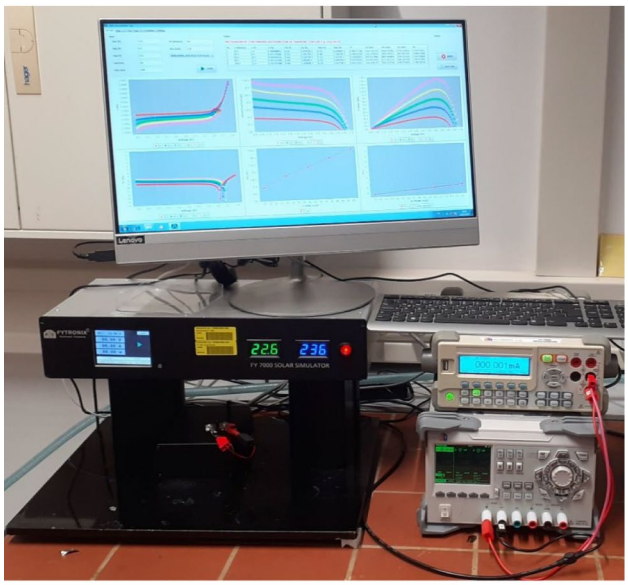

(b)

Fig. 4 (a) An assembled dye-sensitized solar cell with connectors to a multimeter. (b) Characterization of the fabricated solar cell using a solar simulator and source meter.

10.5 mg of ruthenizer 535-bisTBA in 25 mL of ethanol and adding 50.3 mg of chenodeoxycholic acid to the solution. Chenodeoxycholic acid enhances photovoltaic performances of DSSCs in the presence of ruthenium dyes.[40] The TiO_2-coated photoanode was stained with N719 dye by immersing the electrode in the dye solution for 6 h with the white TiO_2 layer facing upwards. Afterwards, the stained electrode was rinsed with ethanol and dried at room temperature. The reference cell, consisting of a TiO_2 electrode stained with N719 dye as sensitizer, the Pt-coated counter electrode, and the iodine/triiodide electrolyte, was assembled and sealed as described above.

The current–voltage characteristics of the fabricated DSSCs were tested under exposure to 1 sun *AM* 1.5 and simulated sunlight of a solar simulator at 100 mW/cm^2 (FY700 Solar Simulator; FY Tronix Electronic) as illustrated in Fig. 4b. The current was measured using an FY700 source meter (FY Tronix Electronic).

Results and Discussion

FTIR Spectrometry Results

The FTIR results displaying the infrared (IR) spectra of the natural dye extracts of *V. amygdalina*, *G. macrosepala* leaves, and *C. ferruginea* are presented in Fig. 5.

The FTIR results in Fig. 5a describe the IR absorbance of the dye extracted from *V. amygdalina* leaves using acetone (VAA) and ethanol (VAE) as solvents. The most noticeable peak in the FTIR result is obtained at 3398 cm^{-1}, with shoulder peaks at 2932 and 2864 cm^{-1}. The FTIR spectra also display peaks at 1717, 1610, 1513, and 1367 cm^{-1}. Other prominent peaks occur at 1261, 1173, and 1027 cm^{-1}. The largest visible peak at 3398 cm^{-1} signifies the presence of a hydroxyl group (OH) or an amine (NH) group in the dye. The peaks at 2932 and 2864 cm^{-1} denote asymmetric and symmetric C-H stretch vibrational modes, respectively, and thus confirm the existence of the alkane group.[41] The bending vibrations at 1717 and 1610 cm^{-1} correspond to the vibrations of the carbonyl (C = O) group in the dye extract. The peak at 1513 represents an aromatic ring stretch (C = C-C) of the aryl group.[42] The peaks at 1367 and 1261 cm^{-1} indicate the O-H bends of the alcohol group, while the peaks at 1173 and 1027 cm^{-1} correspond to the C-N stretch of the amine group. Also, the peaks at 1173 and 1027 cm^{-1} indicate the presence of C-O-C stretch vibrations of acid and carbohydrate groups.[41]

Furthermore, the FTIR results in Fig. 5b illustrate the IR absorbance of the extracted dyes from *G. macrosepala* leaves using acetone (GMA) and ethanol (GME) as solvents. The FTIR results of the two dye samples (GMA and GME) are very similar. The prominent peak in the FTIR spectrometry graph is at 3347 cm^{-1} with shoulder peaks at 2925 and 2849 cm^{-1}. The 1720, 1635, 1522, and 1447 cm^{-1} peaks are also evident, as depicted in Fig. 5b. Other observed absorption peaks occur at 1372, 1165, and 1031 cm^{-1}. The two dye extracts have similar peaks in their respective FTIR spectrograph. The significant difference, however, is that the GME dye extract has more absorbance intensity at 2925 and 2849 cm^{-1}. The prominent peak at 3447 cm^{-1} accounts for the presence of the hydroxyl group (-OH) or the NH amine bonds. The peaks at 2925 and 2849 cm^{-1} are attributed to asymmetric and symmetric C-H stretch vibrations of the alkane group, respectively. The bending vibrations at 1720

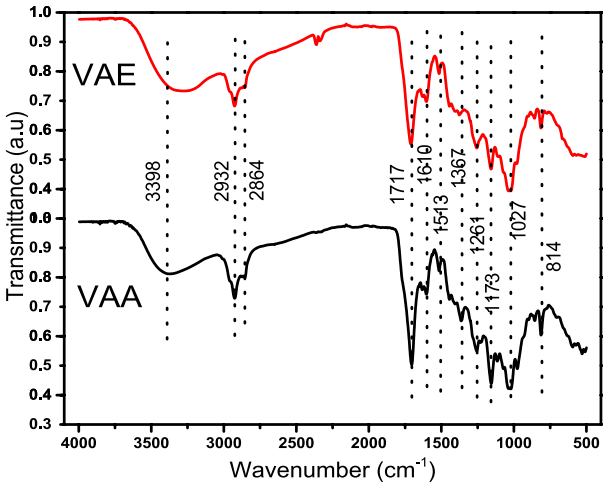

(a)

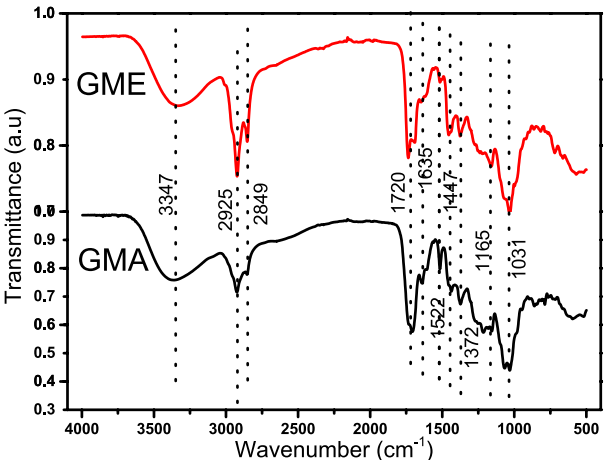

(b)

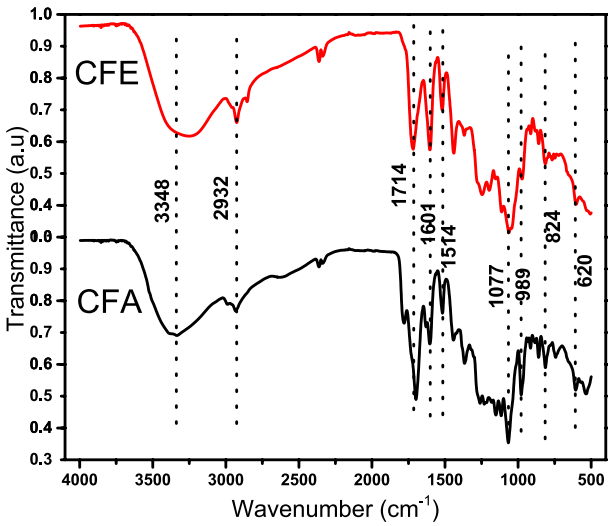

(c)

Fig. 5 Infra-red spectra of the natural dyes extracted from (a) *V. amygdalina* leaves (*VAA* and *VAE*), (b) *G. macrosepala* leaves (*GMA* and *GME*), and (c) *C. ferruginea* fruit (*CFA* and *CFE*), using acetone and ethanol as solvents, respectively.

and 1635 cm^{-1} are associated with the carbonyl (C = O) group, such as carboxylic acid, ketone, and aldehydes. The peaks at 1522 and 1447 cm^{-1} depict the presence of an aromatic ring stretch (C = C-C) of the aryl group, while the peak at 1372 cm^{-1} indicates an O-H bend of the alcohol group. The peaks at 1165 and 1031 cm^{-1} are attributed to the C-N stretch vibrations of the amine group in the dye extract. According to Adedokun et al.[41], the peaks at 1165 and 1031 cm^{-1} also represent the C-O-C stretch vibrations of acid and carbohydrate groups.

Figure 5c describes the IR absorbance of the dye extracted from *C. ferruginea* fruit using acetone (CFA) and ethanol (CFE) as solvents. The major absorption peak recorded at 3348 cm^{-1} corresponds to the hydroxyl group (-OH) or the NH amine bonds, while the shoulder peak at 2932 cm^{-1} confirms the existence of C-H stretching vibrations of the alkane group. The bending vibrations observed at 1714 and 1601 cm^{-1} are characteristics of the carbonyl (C = O) group. Additionally, the peak at 1514 cm^{-1} accounts for the presence of an aromatic ring stretch (C = C-C) of the aryl group, while the peak at 1077 cm^{-1} corresponds to C-O-C stretch vibrations of acid and carbohydrate groups.

According to Isah et al.[43], the presence of the carboxyl functional group (COOH), which comprises both the carbonyl (C = O) and hydroxyl groups, in the *V. amygdalina*, *C. ferruginea*, and *G. macrosepala* dye extracts, promotes better anchoring to the surface of porous TiO_2 film, which results in a strong electronic coupling and rapid forward and reverse electron transfer reactions. The dye anchorage to the surface of a porous semiconductor metal oxide (e.g., TiO_2) film is necessary for effective electron transfer from the dye molecules to the conduction band of the semiconductor oxides.[21] In addition, the IR spectra of the dye extracts consist of bands that can be allocated to the pigment structure observed in the extracts, as depicted in Fig. 5.

UV-Vis Spectrometry Results

The UV-Vis absorption spectra for the natural dye extracts of *V. amygdalina* and *G. macrosepala* leaves are presented in Fig. 6a. According to Fig. 6a, the natural dyes extracted from *V. amygdalina* leaves using acetone (VAA) and ethanol (VAE) as solvents exhibit two major absorption peaks near 410 and 670 mm, which lie in the violet (400–450 nm) and red (625–750 nm) regions, respectively, of the visible light spectrum (400–750 nm). Absorption peaks were also observed near 530 and 610 nm, which correspond to the green (495–570 nm) and orange (590–625 nm) regions of

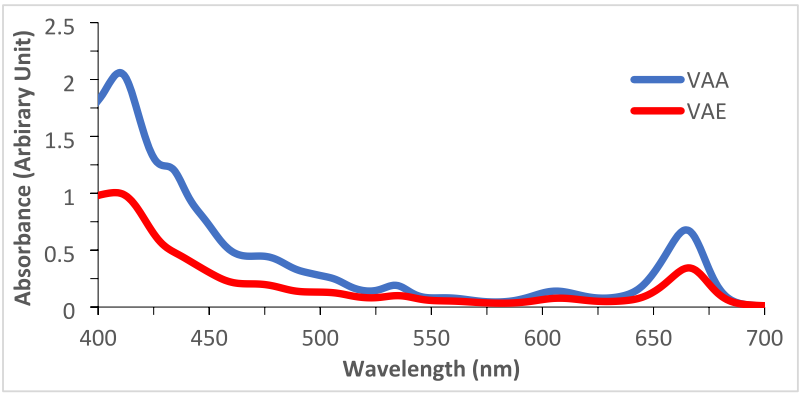

(a)

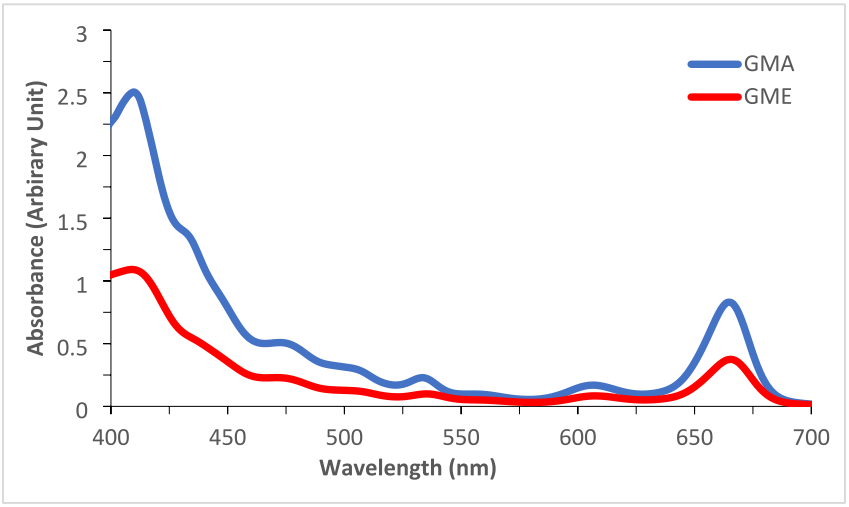

(b)

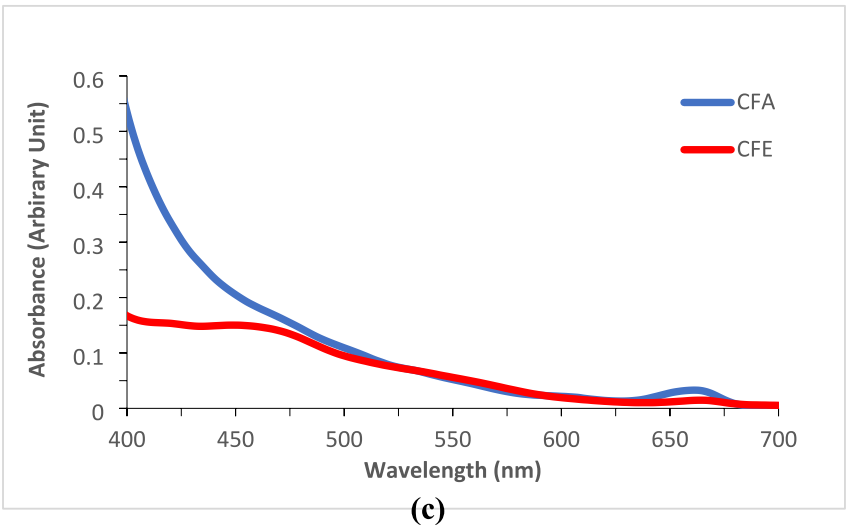

(c)

Fig. 6 UV-Vis absorption spectra of natural dye extracts from (a) *V. amygdalina* leaves (labeled *VAA* and *VAE*), (b) *G. macrosepala* leaves (labeled *GMA* and *GME*), and (c) *C. ferruginea* fruit (labeled *CFA* and *CFE*) , using acetone and ethanol as solvents, respectively.

the visible light spectrum, respectively. This implies that the dye extracts of *V. amygdalina* leaves using acetone and ethanol as solvents could serve as a good photosensitizer in a dye sensitized solar cell because it has a stable absorption of visible light. Based on the UV-Vis spectrometry results, acetone and ethanol are suitable solvents for extracting natural dye from *V. amygdalina* leaves since VAA and VAE demonstrated stable and strong optical absorption in the visible region.

Furthermore, the UV-Vis spectrometry results (Fig. 6b) obtained from the *G. macrosepala* dye extract using acetone (GMA) and ethanol (GME) as solvents show two prominent absorbance peaks near 410 and 665 nm, which fall in the violet and red regions of the visible light spectrum, respectively. Additional absorption peaks were obtained near 480, 535, and 610 nm, which correspond to the blue (450–485 nm), green, and orange regions of the visible light spectrum, respectively, which shows that GMA and GME promise to be suitable DSSC photosensitizers. Therefore, acetone and ethanol are suitable solvents for dye extraction from *G. macrosepala* leaves. Likewise, the UV-Vis absorption spectra for the natural dyes of *C. ferruginea* fruit extracted using acetone (CFA) and ethanol (CFE) display absorption peaks at 400 nm (violet), 460 nm (blue), and 660 nm (red) of the visible spectrum (Fig. 6c). Hence, the dye extracts of *C. ferruginea* fruit using acetone and ethanol as solvents are promising candidates for photosensitizers in DSSCs.

The absorption spectra of *V. amygdalina* and *G. macrosepala* dye extracts (Fig. 6a and b) support the claim that chlorophyll can absorb violet, blue, and red wavelengths and reflect them in green. According to Seithtanabutara et al.[37], the major absorption peaks of chlorophyll in the visible region are typically located at 420 and 660 nm. Additionally, the UV-Vis absorption spectra of all three dyes and their variants using acetone and ethanol as solvents cover a broad range of wavelengths in the visible region of the solar spectrum. The absorption spectra of the natural dyes and their anchorage to the surface of TiO_2 film are crucial to examining the conversion efficiency of the DSSC.

Photoluminescence (PL) Spectroscopy Results

The PL spectra provide details on the photoelectron emission of the natural dye extracts, a factor that determines the photoelectric conversion of a natural dye-based DSSC.[41] In addition, PL spectra are usually studied to understand the recombination of electrons and holes in the dye molecules.[22] The PL spectra of the natural dye extracts of *V. amygdalina* leaves, *C. ferruginea* fruit, and *G. macrosepala* leaves are displayed in Fig. 7. The PL spectra of the three natural dye extracts agree with the UV-Vis absorption spectra of the dye extracts (Fig. 6), while the PL emission peaks, which correspond to high recombination,

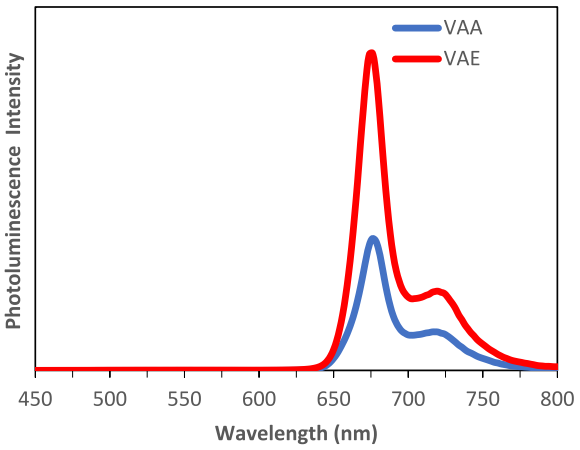

(a)

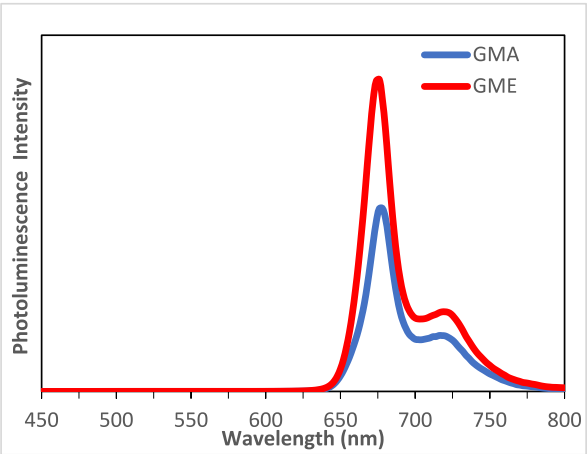

(b)

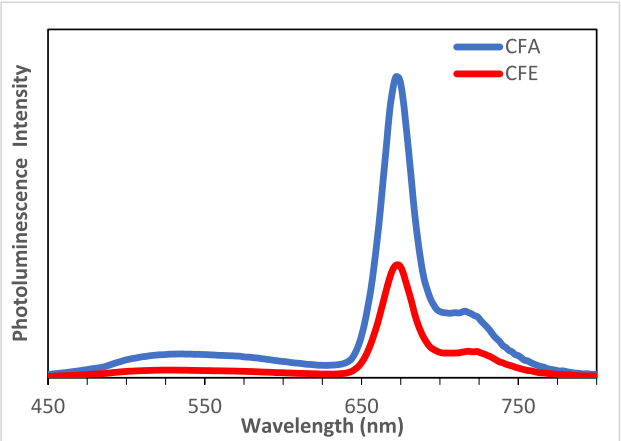

(c)

Fig. 7 Photoluminescence spectra of natural dyes extracted from (a) *V. amygdalina* leaves (labeled *VAA* and *VAE*), (b) *G. macrosepala* leaves (labeled *GMA* and *GME*), and (c) *C. ferruginea* fruit (labeled *CFA* and *CFE*) , using acetone and ethanol as solvents, respectively.

were recorded at different wavelengths for the three dye samples. In the case of the *V. amygdalina* and *G. macrosepala* dye extracts, the maximum fluorescence intensity was centered at 676 nm with an arm at 725 nm, which signifies the characteristic response of chlorophyll.[44] For *C. ferruginea* dye extracts, the PL emission was centered at 550 and 674 nm with an arm at 720 nm, in agreement with the absorption spectra in Fig. 6c. The PL spectra of the acetone-extracted dye samples of *V. amygdalina* and *G. macrosepala* leaves exhibited a lower intensity than those of the ethanol-extracted dye samples (Fig. 6a and b). Thus, natural dye extracts of VAA and GMA would have a lower recombination than those of VAE and GME. In contrast, the ethanol-extracted dye sample of *C. ferruginea* fruit displayed a lower intensity than those of the acetone-extracted dye samples, as illustrated in Fig. 6c, which implies that the natural dye extract of CFE would possess a lower recombination than that of CFA. Therefore, the influence of solvents on the PL spectra of the chlorophyll-based dyes of *V. amygdalina* and *G. macrosepala* leaves differs from that of the anthocyanin-based dye of *C. ferruginea* fruit.

Electrical Properties of DSSCs

The current density–voltage (*J–V*) curves of the DSSCs fabricated using TiO_2 photoanodes sensitized with natural dye extracts of *V. amygdalina*, *G. macrosepala* leaves, and *C. ferruginea* fruit are presented in Fig. 8. The PCE (η) of a solar cell, which is the ratio between maximum power (P_{max}) and incident light power (*Pin*), is calculated by:

$$\eta = \frac{P_{max}}{P_{in}} = \frac{FF \times V_{oc} \times J_{sc}}{P_{in}} \quad (1)$$

where *FF* is the fill factor, V_{oc} is the open-circuit voltage, and J_{sc} is the short-circuit current density.

The fill factor of a solar cell can be calculated by:

$$FF = \frac{P_{max}}{V_{oc} \times J_{sc}} = \frac{V_{max} \times J_{max}}{V_{oc} \times J_{sc}} \quad (2)$$

where V_{max} and J_{max} are the voltage and current density at the maximum power point, respectively.

As displayed by the J–V curves in Fig. 8, DSSCs with natural dye extracts of VAA, VAE, and GMA exhibit higher current densities than those of GME, CFA, and CFE. The

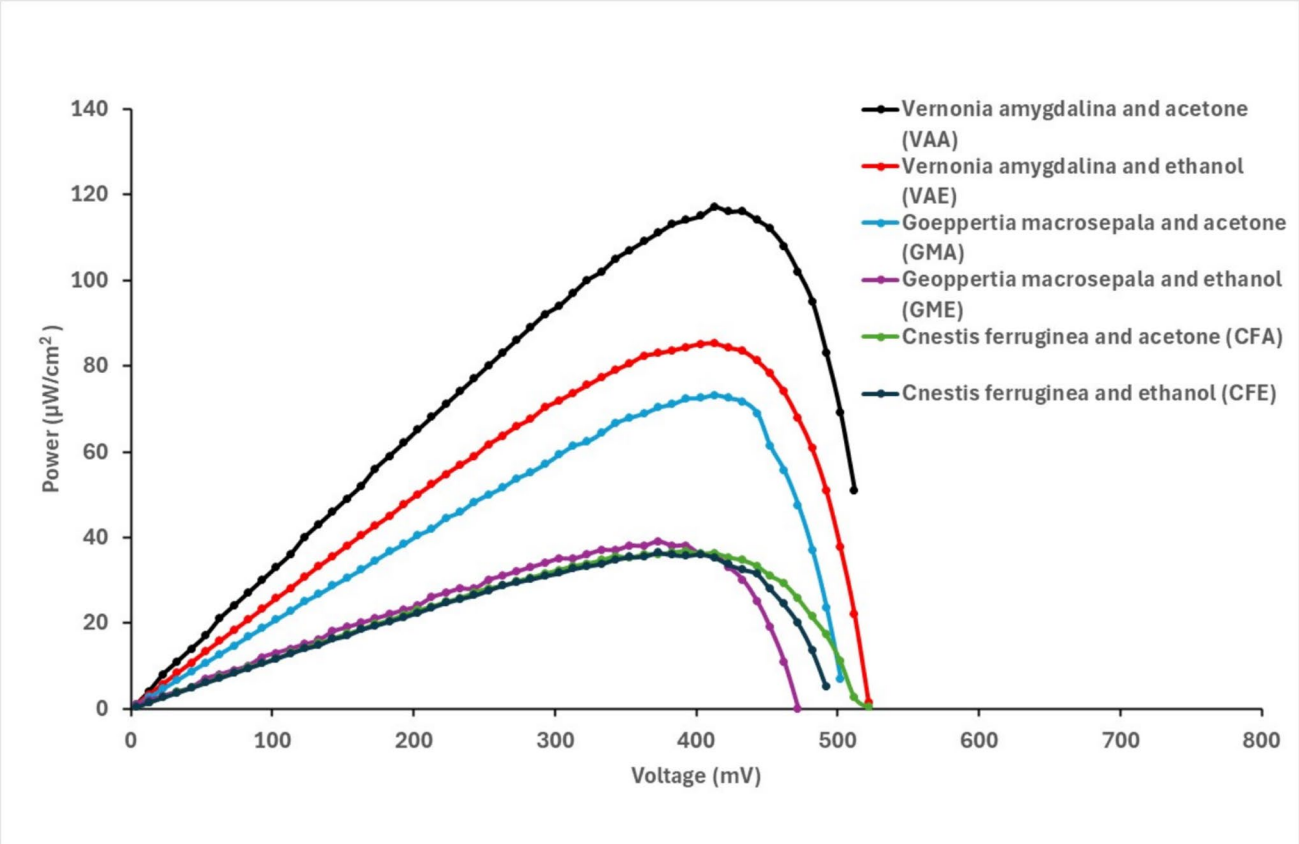

Fig. 8 *J–V* curves of the DSSCs fabricated using TiO_2 photoanodes sensitized with natural dye extracts of *V. amygdalina*, *G. macrosepala* leaves, and *C. ferruginea* fruit.

influence of solvents on the electrical performance parameters (J_{sc}, V_{oc}, FF, and η) of the fabricated DSSCs using natural dye extracts of *V. amygdalina*, *G. macrosepala* leaves, and *C. ferruginea* fruit as photosensitizers are presented in Table I. The performance parameters of the DSSCs fabricated with a synthetic ruthenium-based dye (N719 dye) as the photosensitizer are also included for comparison with those of the natural dyes.

The electrical performance of the two similar devices of each dye-based DSSCs fabricated are contained in Table I and illustrate reproducibility, that is, consistency in the performance of the solar cells. The fabrication process was repeated for each of the natural dye extracts to obtain two solar cells with the same dye as a photosensitizer., and the results show that the performance of both devices of the VAA-, VAE-, GMA-, GME-, CFA-, and CFE-based DSSCs are very similar. Thus, the DSSCs fabricated using TiO_2 photoanodes sensitized with natural dye extracts of *V. amygdalina*, *G. macrosepala* leaves, and *C. ferruginea* fruit are reliable for reproducing a similar performance. Among all the dyes, *V. amygdalina* dyes extracted using acetone (VAA) and ethanol (VAE) offered the highest power conversion efficiencies of 0.12 and 0.09%, respectively, as presented in Table I. Emmanuel et al.[45] reported an efficiency of 0.4% using *V. amygdalina* dye with a nickel dopant, which improved the photochemical performance of the dye. The DSSC fabricated with *G. macrosepala* dye extracted using acetone (GMA) recorded a PCE of 0.07%, while that of *C. ferruginea* fruit (CFA and CFE) displayed a PCE of 0.04%. Hence, the chlorophyll pigments of *V. amygdalina* and *G. macrosepala* leaves produced higher PCE in the fabricated DSSCs than the anthocyanin pigment of *C. ferruginea* fruit. Based on the electrical performance of the natural dye extracts of *V. amygdalina* and *G. macrosepala* leaves as photosensitizers in DSSCs, acetone performed better than ethanol as a solvent for dye extraction by offering greater J_{sc}, V_{oc}, FF, and η compared to ethanol (Table I). The improved performance of the acetone-extracted dyes (VAA and GMA) may be partly due to their lower recombination, as demonstrated by their PL spectra in Fig. 6a and b.

The three natural dyes demonstrated a lower electrical performance than synthetic ruthenium-based dye due to their inherent challenges, such as narrow absorption spectra attributed to their less optimized molecular structures, poor photostability under prolonged illumination, slow electron injection rates, and high recombination losses. The slow electron injection rates can be traced to poor alignment of the highest occupied molecular orbital (HOMO) and lowest unoccupied molecular orbital (LUMO) of the dye which play critical roles in determining the PCE of the DSSC. For effective electron injection, the LUMO of the dye must be higher in energy than the conduction band of TiO_2.[46] If the LUMO is too low, electrons will not efficiently inject into the TiO_2 semiconductor, thereby reducing photocurrent and overall efficiency of the solar cell. Hence, a favorable alignment of HOMO and LUMO levels ensures efficient electron transfer from the dye to the semiconductor and electrolyte, minimizing recombination losses and maximizing the PCE. In addition, the direct transition of the photoexcited electrons from the HOMO to the conduction band of TiO_2 after by-passing the LUMO can be responsible for the low DSSC efficiency obtained with natural dyes as photosensitizers.[47]

The power–voltage (P–V) curves of the DSSCs fabricated using natural dye extracts of *V. amygdalina*, *G. macrosepala* leaves, and *C. ferruginea* fruit as photosensitizers are presented in Fig. 9. A maximum power (P_{max}) of 117 μW/cm^2 was observed for the DSSC fabricated with VAA dye, followed by VAE dye (P_{max} = 85 μW/cm^2) and GMA dye (P_{max} = 73 μW/cm^2).

Table 1 Electrical performance parameters measured for DSSCs fabricated using synthetic and natural dyes as photosensitizers

Dyes	Dye label	Solvent	DSSC samples	J_{sc} (μA/cm^2)	V_{oc} (mV)	FF	η (%)
V. amygdalina leaves	VAA	Acetone	1.1	330.51	522	0.70	0.12
			1.2	308.51	522	0.70	0.11
V. amygdalina leaves	VAE	Ethanol	2.1	253.82	522	0.60	0.09
			2.2	222.58	522	0.60	0.07
G. macrosepala leaves	GMA	Acetone	3.1	208.39	512	0.70	0.07
			3.2	196.67	512	0.70	0.07
G. macrosepala leaves	GME	Ethanol	4.1	127.19	472	0.70	0.04
			4.2	128.93	453	0.60	0.04
C. ferruginea fruit	CFA	Acetone	5.1	120.92	522	0.60	0.04
			5.2	124.00	502	0.60	0.04
C. ferruginea fruit	CFE	Ethanol	6.1	119.17	492	0.60	0.04
			6.2	132.94	482	0.50	0.03
Synthetic dye	N719	Ethanol	7.1	5918.26	702	0.70	2.84
			7.2	5813.91	703	0.70	2.77

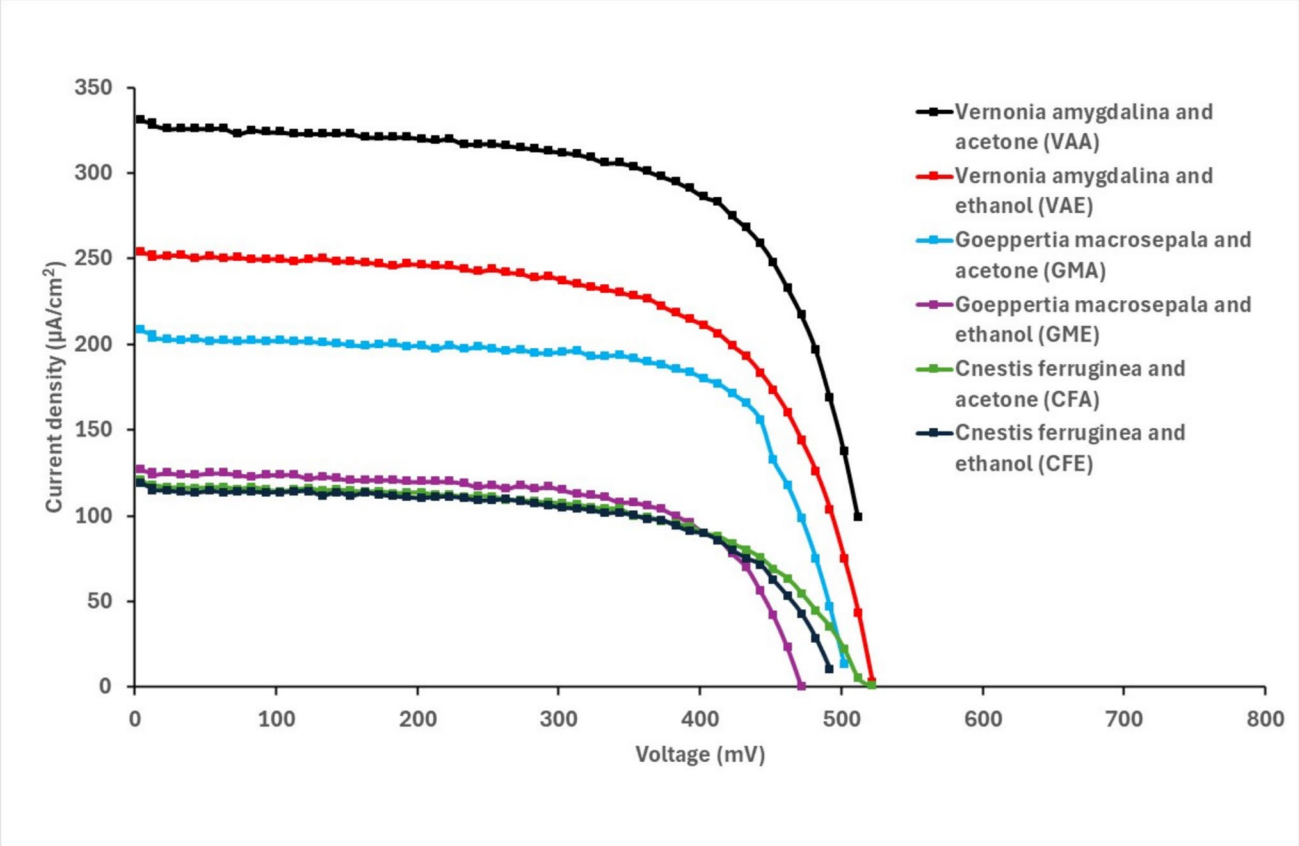

Fig. 9 *P–V* curves of the DSSCs fabricated using TiO_2 photoanodes sensitized with natural dye extracts of *V. amygdalina*, *G. macrosepala* leaves, and *C. ferruginea* fruit.

Conclusions

The performance of DSSCs with natural dye extracts of *Vernonia amygdalina*, *Goeppertia macrosepala* leaves, and *Cnestis ferruginea* fruit as photosensitizers has been investigated. Acetone and ethanol were used for the dye extraction to demonstrate the effects of solvents on the photochemical performance of the natural dyes. The FTIR spectrometry results of *V. amygdalina*, *G. macrosepala*, and *C. ferruginea* dye extracts confirmed the presence of three functional groups—the hydroxyl, amine, and carbonyl groups—a strong indication of good adsorption by the semiconductor metal oxides in the DSSCs, which is necessary for the effective electron transfer from the dye molecules to the conduction band of the semiconductor oxides.

The UV-Vis absorption spectra showed that the natural dye extracts of *V. amygdalina* and *G. macrosepala* leaves absorbed over a wavelength range of 410–680 nm with two prominent absorption peaks near 410 and 670 nm, typical of chlorophyll pigments. *C. ferruginea* dye extracts absorbed at a wavelength range of 400–680 nm with maximum absorption at 400, 460, and 660 nm. The PL spectra of the three natural dye extracts agreed with the UV-Vis absorption spectra of the dyes. For both *V. amygdalina* and *G. macrosepala* dye extracts, a fluorescence intensity peak was obtained at 676 nm with an arm at 725 nm, confirming the presence of chlorophyll. In the case of the *C. ferruginea* dye extracts, the PL emission was centered at 550 and 674 nm with an arm at 720 nm, in agreement with the UV-Vis absorption spectra. With a stable and strong optical absorption in the visible region, acetone and ethanol were suitable solvents for extracting natural dyes from *V. amygdalina*, *G. macrosepala*, and *C. ferruginea*. The absorption spectra also demonstrated that the three natural dyes examined are potential candidates for photosensitizers in DSSCs.

The DSSC fabricated with *V. amygdalina* dye extracted using acetone (VAA) delivered the highest solar efficiency with performance parameters (J_{sc}, V_{oc}, *FF*, and η) of 330.5 μA/cm^2, 522 mV, 0.7, and 0.12%, respectively, closely followed by the VAE dye-based DSSC with characteristic parameters (J_{sc}, V_{oc}, *FF*, and η) of 253.8 μA/cm^2, 522 mV, 0.6, and 0.09%, respectively. In the third position was the DSSC fabricated using *G. macrosepala* dye extracted with ethanol delivering an efficiency of 0.07% with J_{sc}, V_{oc}, and *FF* of 208.39 μA/cm^2, 512 mV, and 0.7. The chlorophyll pigments of *V. amygdalina* and *G. macrosepala* leaves

displayed a higher solar efficiency than the anthocyanin pigment in *C. ferruginea* fruit ($\eta = 0.04\%$). Acetone performed better than ethanol as a solvent for dye extraction from *V. amygdalina* and *G. macrosepala* leaves by offering greater J_{sc}, V_{oc}, *FF*, and η than ethanol. The three natural dyes demonstrated a lower electrical performance than the synthetic ruthenium-based dye ($\eta = 2.84\%$) due to their inherent challenges, such as narrow absorption spectra attributed to their less-optimized molecular structures, poor photostability under prolonged illumination, slow electron injection rates, and high recombination losses. However, optimization of the DSSC performance is achievable through proper molecular engineering of the natural dyes to tune the HOMO and LUMO levels.

Acknowledgment The authors thankfully acknowledge the support of Prof. Niyazi Serdar Sariciftci, Director of Linz Institute for Organic Solar Cells (LIOS), for the research collaboration and manuscript proofreading.

Funding The authors gratefully acknowledge Africa-UniNet funding provided by the Austrian Federal Ministry of Education, Science and Research (Research Grant P091).

Conflict of interest The authors reported no potential conflict of interest

References

1. S. Ashok, Solar energy: description, uses, & facts. *Encyclopedia Britannica,* 2019
2. S. Kohn, D. Wehlage, I. Juhász Junger, and A. Ehrmann, Electrospinning a dye-sensitized solar cell. *Catalysts* 9(12), 975 (2019).
3. M. Kokkonen, P. Talebi, J. Zhou, S. Asgari, S. Soomro, F. Elsehrawy, J. Halme, S. Ahmad, A. Hagfeldt, and S. Hashmi, Advanced research trends in dye-sensitized solar cells. *J. Mater. Chem. A* 9(17), 10527 (2021).
4. H. Michaels, M. Rinderle, R. Freitag, I. Benesperi, T. Edvinsson, R. Socher, A. Gagliardi, and M. Freitag, Dye-sensitized solar cells under ambient light powering machine learning: towards autonomous smart sensors for the internet of things. *Chem. Sci.* 11(11), 2895 (2020).
5. M. Freitag, J. Teuscher, Y. Saygili, X. Zhang, F. Giordano, P. Liska, J. Hua, S. Zakeeruddin, J. Moser, M. Grätzel, and A. Hagfeldt, Dye-sensitized solar cells for efficient power generation under ambient lighting. *Nat. Photonics* 11(6), 372 (2017).
6. J. Barichello, P. Mariani, L. Vesce, D. Spadaro, I. Citro, F. Matteocci, A. Bartolotta, A. Di Carlo, and G. Calogero, Bifacial dye-sensitized solar cells for indoor and outdoor renewable energy-based application. *J. Mater. Chem. C* 12(7), 2317 (2024).
7. A. Ehrmann and T. Blachowicz, Recent coating materials for textile-based solar cells. *AIMS Mater. Sci.* 6(2), 234 (2019).
8. V. Yadav, S. Chaudhary, C.M.S. Negi, and S.K. Gupta, Textile dyes as photo-sensitizer in the dye sensitized solar cells. *Opt. Mater.* 109, 110306 (2020).
9. A.A. Willoughby, A.O. Soge, O.F. Dairo, O.D. Olukanni, E.U. Durugbo, W.S. Michael, and T.A. Adebayo, Fabrication and characterization of a dye-sensitized solar cell using natural dye extract of rosella (*Hibiscus sabdariffa* L.) as photosensitizer. *J. Niger. Soc. Phys. Sci.* 3(4), 287 (2021).
10. A.S. Najm, S.A. Alwash, N.H. Sulaiman, M.S. Chowdhury, and K. Techato, N719 dye as a sensitizer for dye-sensitized solar cells (DSSCs): a review of its functions and certain rudimentary principles. *Environ. Prog. Sustain. Energy* 42(1), e13955 (2023).
11. C.P. Lee, C.T. Li, and K.C. Ho, Use of organic materials in dye-sensitized solar cells. *Mater. Today* 20(5), 267 (2017).
12. A.K. Rajan and L. Cindrella, Studies on new natural dye sensitizers from Indigofera tinctoria in dye-sensitized solar cells. *Opt. Mater.* 88, 39 (2019).
13. N. Sawhney, A. Raghav, and S. Satapathi, Utilization of naturally occurring dyes as sensitizers in dye sensitized solar cells. *IEEE J. Photovolt.* 7(2), 539 (2016).
14. P.M. Sirimanne, M.K.I. Senevirathna, E.V.A. Premalal, P.K.D.D.P. Pitigala, V. Sivakumar, and K. Tennakone, Utilization of natural pigment extracted from pomegranate fruits as sensitizer in solid-state solar cells. *J. Photochem. Photobiol. A* 177(2–3), 324 (2006).
15. M.R. Narayan, Dye sensitized solar cells based on natural photosensitizers. *Renew. Sustain. Energy Rev.* 16(1), 208 (2012).
16. M. Grätzel, Dye-sensitized solar cells. *J. Photochem. Photobiol. C* 4(2), 145 (2003).
17. F. Kabir, S. Sakib, S. Uddin, E. Efaz, and M. Himel, Enhance cell performance of DSSC by dye mixture carbon nanotube and post TiCl4 treatment along with degradation study. *Sustain. Energy Technol. Assess.* 35, 298 (2019).
18. N. Siregar, Motlan, J.H. Panggabean, M. Sirait, J. Rajagukguk, N.S. Gultom, and F.K. Sabir, Fabrication of dye-sensitized solar cells (DSSC) using Mg-doped ZnO as photoanode and extract of rose myrtle (Rhodomyrtus tomentosa) as natural dye. *Int. J. Photoenergy* (2021). https://doi.org/10.1155/2021/4033692.
19. S. Sowmya, N. Ruba, K. Inbarajan, P. Prakash, and B. Janarthanan, Dye-sensitized solar cells concocted with dyes extracted from fresh and dried leaves of Henna using different solvents. *Opt. Quant. Electron.* 53(5), 274 (2021).
20. A. Ali, S.A. Hassan, A. BaQais, and J.S. Binoj, A study on the application of solar cells sensitized with a blackberry-based natural dye for power generation. *J Nanomater.* 2022(1), 2834206 (2022).
21. S.C. Yadav, M.K. Tiwari, A. Kanwade, H. Lee, A. Ogura, and P.M. Shirage, Butea monosperma, crown of thorns, red lantana camara and royal poinciana flowers extract as natural dyes for dye sensitized solar cells with improved efficiency. *Electrochim. Acta* 441, 141793 (2023).
22. A. Mahapatra, P. Kumar, A.K. Behera, A. Sen, and B. Pradhan, Comparative study of natural dye-sensitized solar cells using inedible extracts from kumkum, kamala and malabar spinach fruits. *J. Photochem. Photobiol. A* 436, 114385 (2023).
23. H.V. Flint, H.A.R. Tito, R.D. James, F. Cucinotta, E. Gibson, and M. Caceda, Betanin dye extracted from ayrampo (Opuntia soehrensii) seeds to develop dye-sensitized solar cells. *RSC Adv.* 14(14), 9913 (2024).
24. S. Rakshit, A.K. Karan, and N.B. Manik, Enhanced electrical transport properties of beetroot dye-based thin film in presence of titanium dioxide nanoparticles. *J. Electron. Mater.* 53(7), 3914 (2024).
25. H. Zhou, M. Aftabuzzaman, Masud, S.H. Kang, and H.K. Kim, Key materials and fabrication strategies for high-performance dye-sensitized solar cells: comprehensive comparison and perspective. *ACS Energy Lett.* 10(2), 881 (2025).
26. E. Maruccia, S. Galliano, E. Schiavo, N. Garino, A.Y. Zarate, A.B. Muñoz-García, M. Pavone, C. Gerbaldi, C. Barolo, V. Cauda, and F. Bella, Exploring zinc oxide morphologies for aqueous solar cells by a photoelectrochemical, computational, and multivariate approach. *Energy Adv.* 3(5), 1062 (2024).
27. R. Kumar, A. Umar, G. Kumar, H. Nalwa, and A. Kumar, Zinc oxide nanostructure-based dye-sensitized solar cells. *J. Mater. Sci.* 52, 4743 (2017).

28. R. Vittal and K. Ho, Zinc oxide based dye-sensitized solar cells: a review. *Renew. Sustain. Energy Rev.* 70, 920 (2017).
29. S. Ndlovu, E. Muchuweni, M. Ollengo, and V. Nyamori, Tuning the properties of reduced graphene oxide-$Sr_{0.7}Sm_{0.3}Fe_{0.4}Co_{0.6}O_3$ nanocomposites as potential photoanodes for dye-sensitized solar cells. *J. Electron. Mater.* 52(9), 5843 (2023).
30. A. Dharani, M. Praveen, T. Archana, and R. Kanimozhi, rGO/Ce-Zn_2SnO_4 composite: a high-performance photoanode for enhanced solar energy conversion in dye-sensitized solar cells. *J. Electron. Mater.* 54, 1 (2025).
31. W. Shah, S.M. Faraz, and Z.H. Awan, Photovoltaic properties and impedance spectroscopy of dye sensitized solar cells co-sensitized by natural dyes. *Physica B* 654, 414716 (2023).
32. H. Chang and Y. Lo, Pomegranate leaves and mulberry fruit as natural sensitizers for dye-sensitized solar cells. *Sol. Energy* 84(10), 1833 (2010).
33. Bitter leaf (Vernonia amygdalina), Wikipedia, 19 June 2024. Available: https://en.wikipedia.org/wiki/Vernonia_amygdalina. Accessed 4 September 2024
34. E.O. Farombi and O. Owoeye, Antioxidative and chemopreventive properties of Vernonia amygdalina and Garcinia biflavonoid. *Int. J. Environ. Res. Public Health* 8(6), 2533 (2011).
35. "Goeppertia macrosepala, Plants of the World Online," Board of Trustees of the Royal Botanic Gardens, Kew, 2023. Available: https://powo.science.kew.org/taxon/urn:lsid:ipni.org:names:60461039-2. Accessed 4 September 2024
36. H.A. Ahmed, Therapeutic potentials of Cnestis ferruginea: a review. *J. Pharmacogn. Phytochem* 6(6), 1397 (2017).
37. V. Seithtanabutara, N. Chumwangwapee, A. Suksri, and T. Wongwuttanasatian, Potential investigation of combined natural dye pigments extracted from ivy gourd leaves, black glutinous rice and turmeric for dye-sensitised solar cell. *Heliyon* 9(11), e21533 (2023).
38. S. Hao, J. Wu, Y. Huang, and J. Lin, Natural dyes as photosensitizers for dye-sensitized solar cell. *Sol. Energy* 80(2), 209 (2006).
39. A. Shrivastava, E. M. Dedhia, M. Daniel, S. Bhattacharya, and Arya, in *Extraction and dyeing methods for natural dyes*, Natural dyes: scope and challenges (2006), pp 67-80
40. Solaronix, Materials catalogue, Solaronix Ltd, 2024, pp. 14-16.
41. O. Adedokun, Y.K. Sanusi, and A.O. Awodugba, Solvent dependent natural dye extraction and its sensitization effect for dye sensitized solar cells. *Optik* 174, 497 (2018).
42. J. Coates, Interpretation of infrared spectra, a practical approach. *Encycl. Anal. Chem.* 12, 10815 (2000).
43. K.U. Isah, A.Y. Sadik, and B.J. Jolayemi, Effect of natural dye co-sensitization on the performance of dye-sensitized solar cells (DSSCs) based on anthocyanin and betalain pigments sensitisation. *Eur. J. Appl. Sci.* 9(3), 140 (2017).
44. W.H. Lai, Y. Hsun, L.G. Teoh, and M.H. Hona, Commercial and natural dyes as photosensitizers for a water-based dye-sensitized solar cell loaded with gold nanoparticles. *J. Photochem. Photobiol. A* 195(2–3), 307 (2008).
45. O.C. Emmanuel, O.N. Donald, and I.L. Ikhioya, Effect of doping and Co-sensitization on the photovoltaic properties of natural dye-sensitized solar cells. *SSRG Int. J. Appl. Phys.* 9(3), 44 (2022).
46. M. Ben Karoui, S. Saadaoui, A. Torchani, and R. Gharbi, Effect of natural sensitizers anchoring to nanoporous TiO_2 on performance of dye-sensitized solar cells. *J. Electron. Mater.* 50(8), 4797 (2021).
47. Y.C. Chen and J.T. Lin, Multi-anchored sensitizers for dye-sensitized solar cells. *Sustain. Energy Fuels* 1(5), 969 (2017).